Supplemental material for generation of atmospheric turbulence with unprecedentedly large Reynolds-number in a wind tunnel

EXCITATION

We first discuss the shaft-dependence of the active grid. Indeed, the shaft dependencies allow to define the individual shaft motion by one stochastic time series. Neighboring shafts turn in opposite directions to ensure an undirected flow.

Most importantly the global blockage of the grid is kept constant. Thereto, the active grid is split into two groups, which are compensating each others local blockage change. One group is following the stochastic input time series α. The other group is compensating the local blockage change by following

$$\beta = \arcsin\left((\sin\left(|\alpha|\right) - 1 - \sin\left(\gamma\right)) \cdot N_\alpha / N_\beta\right), \quad (1)$$

with the corresponding number of shafts per group N_α and N_β and an offset γ to keep the central shaft angle around 30°. In our definition, 0° correspond to an open position where the flaps are aligned with the flow, and 90° correspond to a position where the flaps are perpendicular to the main flow direction.

The groups in this case are defined as an inner group (inner 10 shafts vertical and horizontal) and an outer group (outer 5 shafts per side). Hereby the shafts of the inner group (roughly 1.5 m x 1.5 m core) are directly correlated, and the same is true for the outer shafts. Furthermore, the shafts of the outer group and inner group are correlated by the definition of β. This is leading to a super-position of an excitation by the design of the grid, the separation into different groups, which may be imprinting a grid with a larger spacing, the active grid and the the fan control.

A stochastic time series is used with a scaling based on the Langevin equation

$$\alpha(t+\tau) = \alpha(t) + \tau D_1(\alpha(t)) + \sqrt{\tau D_2(\alpha(t))}\Gamma(t), \quad (2)$$

with the drift term $D_1(\alpha) = -4\alpha$, the diffusion term $D_2(\alpha) = 1$ and Gaussian distributed white noise Γ. The time series is scaled to a mean flap angle of $\overline{\alpha} = 40°$ and a standard deviation of $\sigma(\alpha) = 10°$. The resulting spectrum of the scaled time series $\alpha(t)$ is given in Fig. 1. The fan speed is dynamically varied based on a comparable time series, but at a lower frequency. The fluctuations in the low frequency region of the PSD can be found in the stochastic input as well as in the measured spectra, indicating that those fluctuations are directly caused by the stochastic time series of the excitation.

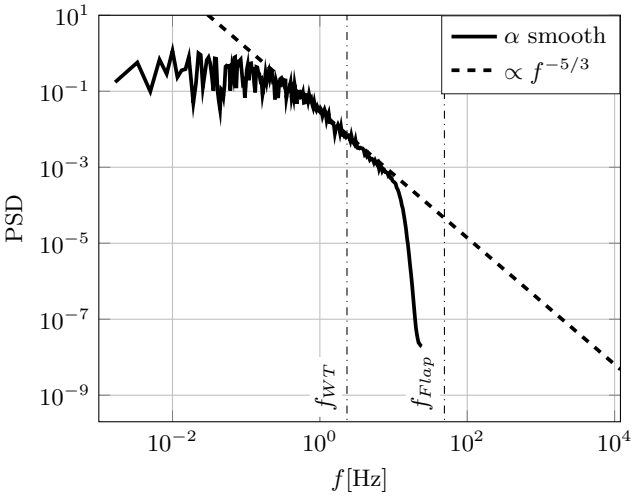

FIG. 1. Exemplary power spectral density of the excitation protocol of the active grid.

ISOTROPY

To give further details about the generated flows, the transversal component of the velocity is investigated. Results are shown for the case including the dynamic fan speed variation.

Fig. 2 shows the power spectral density of the longitudinal and transversal component of the flow for an excitation by the active grid and the wind tunnel fan. Both spectra show a good agreement for frequencies larger than $f_{WT} := \frac{\overline{u}}{L_{WT}}$, defined with the wind tunnel size $L_{WT} = 3\,\mathrm{m}$ and the mean wind speed $\overline{u}$. Deviations are found for smaller frequencies. Hence, the wind tunnel size does limit the fluctuations of the transversal component, but not of the longitudinal component.

Fig. 3 shows the shape factor λ^2 of the longitudinal and transversal component of the flow for an excitation by the active grid and the wind tunnel fan. Again, on the small scales, a similar behavior of both components can be observed. For scales larger than $T_{WT} := \frac{L_{WT}}{\overline{u}}$, the longitudinal component becomes Gaussian ($\lambda^2 = 0$). For the transversal component, still higher λ^2 values can be found for scales larger than T_{WT}.

Interestingly, at small scales the λ^2 of the transversal component shows about the same intermittency as the one of the longitudinal component, whereas the power spectrum for the transversal component saturates. Taking λ^2 as a parameter, which corresponds to the depth of the cascade, we conjecture that the transversal cascade starts at a similar depth/intermittency as the longitudinal cascade for this scale - this supports our statement

of a slice cut out of much-larger-scale turbulence.

The analysis of the transversal velocity component is showing comparable results for time scales up to 0.5 s. This is indicating approximate isotropy in the small scales (Fig. 2, 3). The highest isotropy is found at scales of roughly 1 m. The anisotropy for larger scales behaves in a way also observed by [1]. Hence, the flow exhibits turbulence properties comparable to those found in the atmospheric boundary layer.

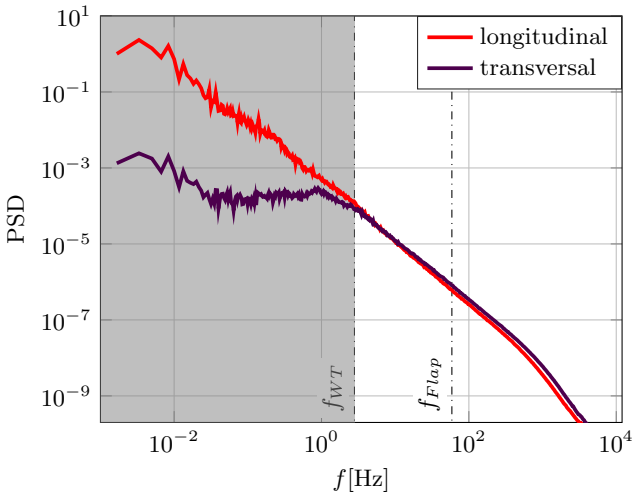

FIG. 2. Longitudinal and transversal power spectral density of the excitation by active grid and wind tunnel fans. The gray region marks scales larger than the wind tunnel width.

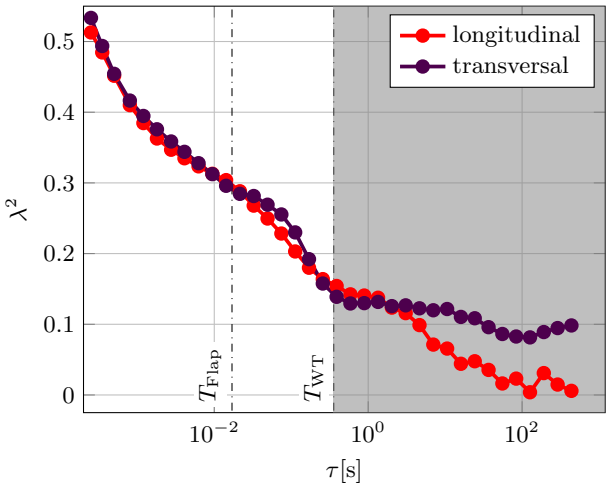

FIG. 3. Shape factor λ^2 for the longitudinal and transversal component of the excitation by active grid and wind tunnel fans. The gray region marks scales larger than the wind tunnel width.

HOMOGENEITY

To compare the flow at different positions in a cross sectional region of the wind tunnel the results of two hot wires are compared (Fig. 4, 5). One hot wire is placed in the centerline and one shifted diagonal by roughly 0.425 m at a downstream position of roughly 126M.

The mean wind speed measured in the centerline is 6.91 m s^{-1} and the one of the shifted measurement is 6.96 m s^{-1}. The turbulence intensities are 15.6% and 15.3%, respectively. Hence, the deviation between both positions is below 2%.

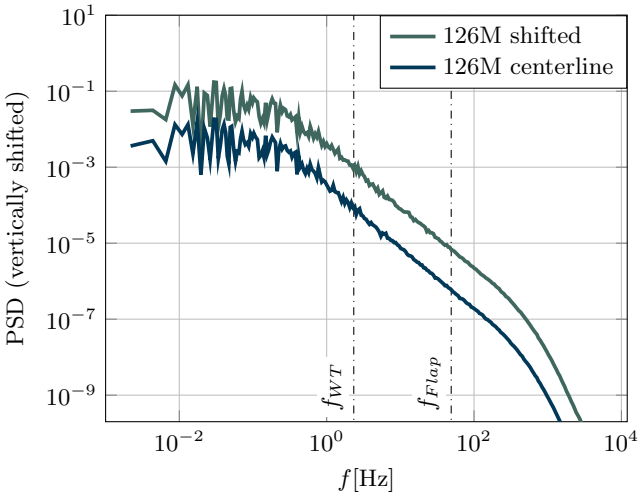

FIG. 4. Power spectral density measured by one hot-wire in the centerline and one shifted diagonal in the cross section by 0.425 m for the excitation by the active grid.

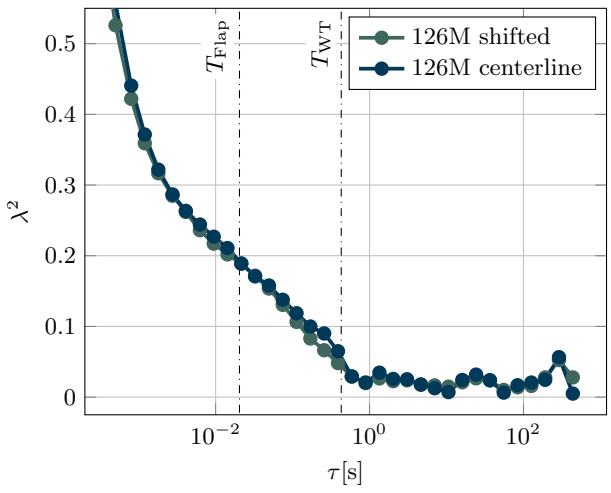

FIG. 5. Shapefactor λ^2 for measurements by one hot-wire in the centerline and one shifted diagonal in the cross section by 0.425 m for the excitation by the active grid.

Fig. 4 shows the power spectral density for both hot wires (the PSD of the shifted hot wire is vertically shifted). Both position show a comparable spectra.

Fig. 5 shows the shape factor λ^2 for both hot wires. Again, both measurements show comparable shape factors.

The analysis of the transversal shifted hot wire is showing comparable results on all scales. In the investigated core region of the wind tunnel a homogeneous flow can be assumed (Fig. 4, 5).

KINETIC ENERGY BALANCE

Grid-turbulence is created by generating perturbations which then develop into turbulence. Let us call the initially imposed perturbations U_i and the developed self-organized turbulent fluctuations u_i. The associated turbulent kinetic energy is

$$k = \frac{1}{2}\overline{u_i u_i}. \tag{3}$$

The balance for k writes,

$$d_t k = p - \epsilon, \tag{4}$$

where p is given by

$$p = \overline{u_i u_j} D_{ij}, \tag{5}$$

where $D_{ij} = (\partial_i U_j + \partial_j U_i)/2$. Using a classical eddy-viscosity assumption, we can write p as

$$p = \nu_T D_{ij} D_{ij}, \tag{6}$$

where ν_T is determined by the turbulent fluctuations u_i. A classical grid induces mainly transverse fluctuations of the stream-wise velocity, leading to

$$p \sim \nu_T \frac{U_x^2}{M^2}, \tag{7}$$

where M is the transverse correlation size of the turbulent fluctuations, and U_x is set by the velocity deficit in the grid-bar-wakes. Streamwise modulation adds a second term to the production, leading to

$$p \sim \nu_T \left(\frac{U_x^2}{M^2} + \frac{U_y^2}{L^2} \right), \tag{8}$$

where L is the longitudinal correlation length of the transverse fluctuations induced by the modulation of fan and active grid. The length L, since it is longitudinal, is not constrained by the width of the wind tunnel. If the size of the perturbations U_y is large enough, this contribution to the kinetic energy balance allows the injection of kinetic energy into the turbulence at typical scales of order L.

Evidently, this order-of-magnitude estimate does not take into account the detailed multi-scale nature of the injection, but only shows, on the level of integral quantities, how the large scales are affected by transverse and longitudinal shear-layers, with given correlation-lengths.

[1] C. Klipp, Boundary-layer meteorology **151**, 57 (2014).